Journal of Thermal Analysis and Calorimetry, Vol. 82 (2005) 477–481

HOW THERMOTROPIC PROPERTIES INFLUENCE THE FORMATION OF LYOTROPIC AGGREGATES NEAR THE CRITICAL MICELLE CONCENTRATION

V. M. Garamus[1], *G. E. Milkereit*[2], *Regine Willumeit*[1] *and V. Vill*[2*]

[1]GKSS Research Centre, Max-Planck-Str.1, 21502 Geesthacht, Germany
[2]Institute of Organic Chemistry, University of Hamburg, Martin-Luther-King-Platz 6, 20146 Hamburg, Germany

In this work, we investigated the lyotropic aggregation behaviour in dilute solutions of two synthetic glycolipids with same alkyl chain. The chemical structure of the carbohydrate headgroups is similar, nevertheless as reported the thermotropic phase behaviour is different. We found that the slightly tilted compound showing a complex thermotropic phase behaviour forms large aggregates with substructure already in dilute solutions and the significantly tilted compound with its simple thermotropic phase behaviour forms small spherical micelles near the CMC.

Keywords: *glycolipids, lyotropic aggregation, SAXS, thermotropic phase behaviour*

Introduction

In recent years, glycolipids have gained much interest in biophysics and physical chemistry. The biological interest focuses on their role in cell membranes and cell fusion processes. Simple alkyl glycosides can be found as membrane components [1], whereas more complex glycolipids are reported to serve as second messengers [2], pathogens [3–7] and some are substructures of complex endotoxines [8–10]. Especially, the type of carbohydrate headgroup plays an important role in cell recognition and membrane fusion processes [11–16].

From the industrial point of view, the surfactants from renewable sources are important ingredients for consumer health, and care products. Especially, alkyl glycosides and alkyl polyglucosides are the major group of this new natural surfactants [17–20].

Furthermore, many of the features of the self-aggregation of ionic and PEO-based surfactants are difficult or impossible to apply to alkyl glycosides in a direct and meaningful manner. More specifically, alkyl glycosides carry no charge but still have rigid carbohydrate headgroups. Therefore, they share features with PEO-based and ionic surfactants. In addition, the chirality of carbohydrate head groups has a great influence on the self-assembly in solutions [21].

Generally, the calorimetric effects of the dilute glycolipid–water systems are hardly detectable [22]. In this issue the concentrated endotoxine/phospholipid/water is described by Urban *et al*. and showed that in the case of the abundance of endotoxine the calorimetric effects are vanished (the temperature range of the phase transition is extended extremely and the change in enthalpy is reduced drastically) in spite the fact that significant structural changes occur during the increasing temperature [23]. We have intend to show that the thermotropic behaviour of the dilute glycolipid system with minor thermotropic effect is accompanied with complex structural formation which are observed by using scattering technique. The thermotropic properties of

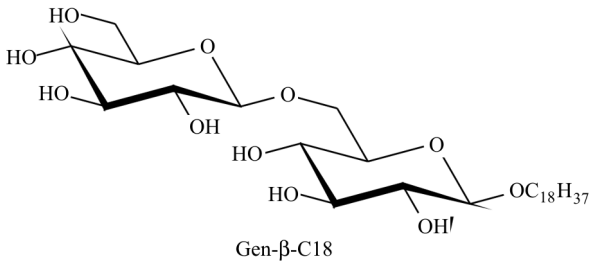

Fig. 1 Chemical structures of the investigated lipids Gen-β-C18 and Mel-α-C18

* Author for correspondence: vill@chemie.uni-hamburg.de

1388–6150/$20.00

Akadémiai Kiadó, Budapest, Hungary
Springer, Dordrecht, The Netherlands

both compounds were already investigated by polarizing microscopy [24]. Mel-α-C18 shows only thermotropic Smectic A phase whereas Gen-β-C18 shows thermotropic Smectic A and cubic phases. The structure of the slightly wedge-shaped Gen-β-C18 is subject to the conflict between the hydrophilic and hydrophobic moiety, where the carbohydrate head favours the formation of columnar structures and the lipophilic tail favours the formation of lamellar structures which results in the formation of cubic phases besides the smectic phase. This structural conflict also destabilises the phase range of the liquid crystalline phase compared to the melibioside Mel-α-C18, which shows liquid crystalline phase behaviour over a temperature range of 122°C whereas the Gen-β-C18 shows a liquid crystalline phase only over a temperature interval of 98°C.

Small angle neutron scattering data were collected for solutions of Gen-β-C18 at 25°C and for Mel-α-C18 solutions at 50°C in D_2O. The higher temperature for second compound is applied with purpose to increase the solubility of Mel-α-C18 and to improve signal/noise ratio in scattering experiments.

In this work, we investigated the lyotropic aggregation behaviour in dilute solutions of synthetic glycolipids with different molecular shapes: slightly wedge-shaped (Gen-β-C18), and significantly tilted (Mel-α-C18). We found that a rich thermotropic phase behaviour of Gen-β-C18 is connected with formation of complex aggregates already in dilute solution, whereas a lipid Mel-α-C18 showing a simple thermotropic phase behaviour forms only small micelles in dilute solution.

Experimental

Materials and methods

Compounds

Synthesis of the compounds is described elsewhere [24]. Purity of the compounds was estimated to be >99%. Shortcuts are used to describe the compounds within the text: Mel-α-C18 for stearyl 6-O-(α-*D*-galactopyranosyl)-α-*D*-glucopyranoside, and Gen-β-C18 for stearyl 6-O-(β-*D*-glucopyranosyl)-β-*D*-glucopyranoside.

Small angle neutron scattering

Small angle neutron scattering experiments were performed with the SANS-1 instrument at the FRG1 research reactor at the GKSS Research Centre, Geesthacht, Germany [25]. Four sample-to-detector distances (from 0.7 to 9.7 m) were employed to cover the range of scattering vectors q from 0.005 to 0.25 $Å^{-1}$. The neutron wavelength, λ, was 8.1 Å with a wavelength resolution of 10% (full-width-at-full-maximum). The solutions were prepared in D_2O (Deutero GmbH, purity 99.98 %). The samples were kept in quartz cells (Hellma) with a path length of 5 mm. The samples were placed in a thermostated holder, for isothermal conditions: T=25.0±0.5 and 50.0±0.5°C. The raw spectra were converted to an absolute scale and corrected for the backgrounds [26].

Results and discussion

Compounds

The chemical structures of the investigated compounds are shown in Fig. 1. The slightly wedge-shaped compound, Gen-β-C18, is a disaccharide with β-linkage of the alkyl chain and a glucopyranoside moiety linked β1→6 to the first sugar ring. On the other hand, the tilted compound, Mel-α-C18, bears a galactopyranoside moiety linked α1→6 to the first sugar ring. In this lipid, the alkyl chain is linked via an α-glycosidic bond to the disaccharide headgroup.

Analysis of SANS data

SANS data were collected for solutions of Gen-β-C18 (c=1.0·10^{-4}, 5.0·10^{-4}, 1.0·10^{-3} g mL^{-1}) at 25°C, and Mel-α-C18 (c=6.3·10^{-4} g mL^{-1}) at 50°C in D_2O, these concentrations are near the CMC (CMC<1·10^{-5} g mL^{-1} for both compounds).

The obtained scattering curves are very different for the two glycosides (Fig. 2). Compound Gen-β-C18 shows a significant and rapidly decreasing scattering ($d\Sigma(q)/d\Omega \sim q^{-\alpha}$, α=1–2) at the low and intermediate intervals of the scattering vector (q<0.1 $Å^{-1}$). At large values of the scattering vector, q, a diffraction maximum

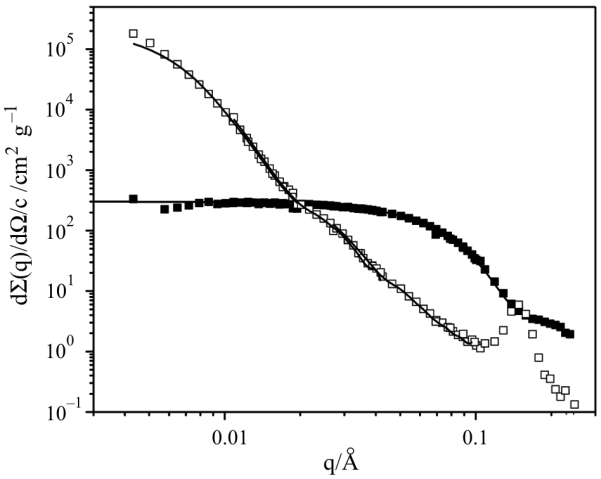

Fig. 2 Scattering curves and model fits for solutions of Gen-β-C18 (□ – c=1.0·10^{-3} g mL^{-1}) and Mel-α-C18 (■ – c=6.3·10^{-4} g mL^{-1}) in D_2O. The curves are normalized to the concentration of the surfactant in micelles. The solid lines represent fits by the IFT method

($q \approx 0.15$ Å^{-1}) can be observed. In contrast to the scattering curve of the Gen-β-C18 solution, the Mel-α-C18 scattering curve shows a small and approximately constant scattering at the low and intermediate intervals of q. It can be assumed that the two lipids form different aggregates in aqueous solution: *i*) Gen-β-C18 forms large aggregates with well-ordered plane or disc-shaped substructures; *ii*) Mel-α-C18 forms small and near spherical aggregates.

We started the analysis of the scattering data by applying the indirect Fourier transformation (IFT) method developed by Glatter [27] in the version of Pedersen [28]. This independent model approach needs only minor additional information about the possible aggregate structure: dimensions (sphere-like, rod-like or disc-like), and a maximum value of the diameter, cross section diameter or thickness, respectively. The IFT routine for spherical-like aggregates was applied to the whole q range of Mel-α-C18 scattering data. Only the low and intermediate (q<0.1 Å^{-1}) q range of the scattering data of Gen-β-C18 were analysed. In the latter case, we have tried to exclude the diffraction maximum from our analysis (q_{max}=0.15 Å^{-1}).

The scattering intensities ($d\Sigma(q)/d\Omega$) of the studied solutions are written via the pair distance distribution function $p(r)$. This is connected with the distribution of the scattering length density within the particles as an autocorrelation function [29]:

$$p(r) \sim \int \Delta\rho(r')\Delta\rho(r+r')dr' \quad (1)$$

where $\Delta\rho(r)$ represents the contrast (difference between the scattering length density of aggregates at the point r, $\rho(r)$, and the averaged scattering length density of the solvent, ρ_s, $\Delta\rho(r)=\rho(r)-\rho_s$.

In the IFT approach, the pair distance distribution function is expressed as a sum of N b-splines, evenly distributed in the interval [0, D_{max}]. The values of the coefficients are calculated numerically by a least square fitting of the IFT model curve to the experimental data. In the present study, the values of D_{max} were carefully chosen to give both, good fits to the experimental data and smooth $p(r)$ functions. In the investigated q range the experimental data and the fitted curves coincide very well (Fig. 2).

The gaussian shape (Fig. 3) of the pair distribution function is characteristic for an almost spherical aggregate formed by compound Mel-α-C18. From the maximum distance of the $p(r)$ function a first estimation of the diameter (~70 Å) is possible. The shape of the $p(r)$ function of compound Gen-β-C18 on the other hand side is determined in a significant larger interval of r (~1000 Å) and suggests a slightly non-symmetrical shape of aggregates. The measured q-range is limited, therefore, it is not possible to investigate the whole size of the aggregates, the diameter of the formed aggregates is larger than 1000 Å, and the system can be polydispersed and/or non-spherical.

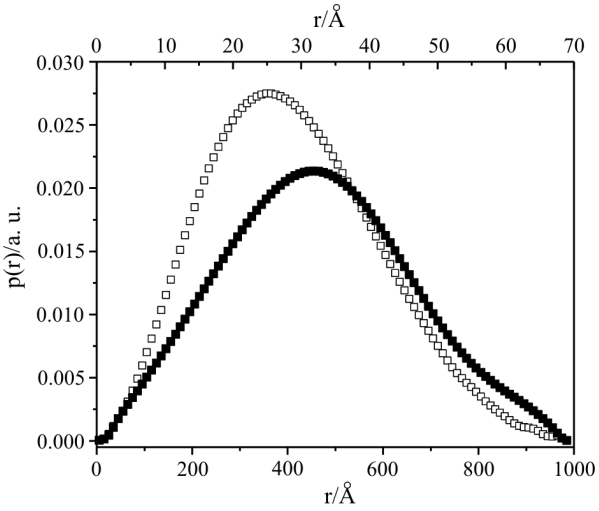

Fig. 3 Pair distance distribution functions obtained for Mel-α-C18 aggregates (■ – r-scale is in the top, D_{max}=70 Å) and for Gen-β-C18 (□ – r-scale is in the bottom, D_{max}=1000 Å)

After determination of the pair distance distribution function, the radius of gyration of the cross section of the aggregates, R_g, can be calculated. The radius of gyration is written in the form:

$$R_g = \left[\frac{\int_0^\infty r^2 p(r)dr}{2\int_0^\infty p(r)dr} \right]^{1/2} \quad (2)$$

The radii of gyration were calculated: *i*) compound Mel-α-C18 – R_g=25.0±0.8 Å (the corresponding radius of the homogeneous sphere is 32±1 Å); *ii*) Compound Gen-β-C18 – R_g=320±8 Å (the corresponding radius of the homogeneous sphere is 410±10 Å).

The analysis was continued by fitting of the Mel-α-C18 scattering data to a spherical model [29]. For the radius of the sphere a value of 31±1 Å was obtained, which agrees with the value obtained from the IFT analysis.

The diffraction maximum at a large q region points on some well-ordered substructures formed by Gen-β-C18 in the concentration range from 10^{-4} to 10^{-3} g mL^{-1}. An increase of the concentration of Gen-β-C18 by a factor of 10 does not change the shape of the scattering curve at a low and intermediate q range (q<0.1 Å^{-1}) as can be seen from Fig. 4. There is no shift of the peak position of the maximum but the peak becomes sharper with increasing concentration. From the position of the peak it is possible to calculate the distance d between the layers using $q_{max}d=2\pi$

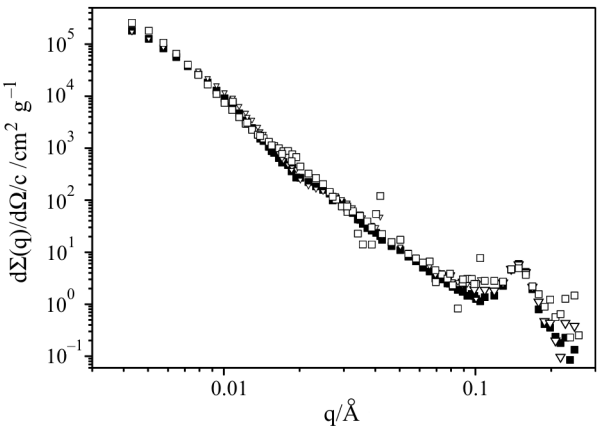

Fig. 4 Scattering curves of Gen-β-C18 solutions in D_2O at different concentrations of the lipid (■ – c=1·10^{-3} g mL^{-1}, ▽ – c=5·10^{-4} g mL^{-1}, □ – c=1·10^{-4} g mL^{-1}, T=25°C)

(d~43 Å). The length of Gen-β-C18 molecules can be calculated from the value of d. The length for one molecule in the layer (21.5 Å) points on a flexible conformation of the alkyl chain. This way of determination of molecular length can be considered only as maximum value of molecular length due to presence of hydrated water. Actually length of molecule is smaller and this supports more our conclusion on flexible conformation of alkyl chain of Gen-β-C18.

The other thermotropic properties of both compounds were already described [24]. Mel-α-C18 shows only thermotropic Smectic A phase whereas Gen-β-C18 shows thermotropic Smectic A and cubic phases. Also the lyotropic structures at a concentration of 0.1 g mL^{-1} were investigated for both compounds by small angle X-ray scattering (SAXS) [28]. At this high concentration, both compounds form lamellar structures in a broad temperature range. SANS-experiments were performed at a concentration near the CMC that is about 10^2 to 10^3 times lower than the concentrations that were used for the SAXS-measurements. At this low concentration where the interaction between aggregates can be neglected a strong influence of the molecular shape on the aggregation behaviour is observed. The significantly tilted melibioside Mel-α-C18 is packed into spherical micelles, here the imbalance between the hydrophilic and hydrophobic moiety is large, whereas in the pure state this imbalance is small, as can be seen from the thermotropic phase behaviour. On the other hand, the slightly wedge-shaped gentibioside, Gen-β-C18, is subject to the conflict between the hydrophilic and hydrophobic moiety, where the carbohydrate head favours the formation of columnar structures and the lipophilic tail favours the formation of lamellar structures. From the thermotropic properties, this can be seen in the formation of a cubic phase besides the Smectic A phase. In dilute solution, this effect decreases resulting in the formation of large disc-like aggregates, because a wedge-shaped structure would favour spherical or cylindrical structures and a rod-like structure the formation of bilayers. Hence large bilayer structures (discs) are formed as a tribute to the slightly tilted structure. With increasing concentration the interaction between the aggregates will be superior and besides other phases the lamellar phase with its bilayer structure dominates the lyotropic phases.

References

1 I. Ishizuka and T. Yamakawa, 1985. Glycolipids, In: H. Wiegandt, (Ed.), New Comprehensive Biochemistry, Elsevier, Vol. 10 (1985), p. 101.
2 S. Schutze, K. Potthoff, T. Machleidt, D. Berkovic, K. Wiegmann and M. Kronke, Cell, 71 (1992) 765.
3 F. Wagner, S. Rottem, H.-D. Held, S. Uhlig and U. Zähringer, Eur. J. Biochem., 267 (2000) 6276.
4 K. Matsuda, T. Kasama, I. Ishizuka, S. Handa, N. Yamamoto and T. Taki, J. Biol. Chem., 269 (1994) 33123.
5 K. Matsuda, I. Ishizuka, T. Kasema, S. Handa, N. Yamamoto and T. Taki, Biochim. Biophys. Acta, 1349 (1997) 1.
6 U. Zähringer, F. Wagner, E. Th. Rietschel, G. Ben-Menachem, J. Deutsch and S. Rottem, J. Biol. Chem., 272 (1997) 26262.
7 K. Matsuda, R. Harasawa, J. L. Li, T. Kasama, T. Taki, S. Handa and N. Yamamoto, Microbiol. Immunol., 39 (1995) 307.
8 U. Seydel, M. H. J. Koch and K. Brandenburg, J. Struct. Biol., 110 (1993) 232.
9 K. Brandenburg, W. Richter, M. H. J. Koch, H. W. Meyer and U. Seydel, Chem. Phys. Lipids, 91 (1998) 53.
10 K. Brandenburg, M. H. J. Koch and U. Seydel, J. Struct. Biol., 105 (1990) 11.
11 W. Curatolo, Biochim. Biophys. Acta, 906 (1987) 111.
12 V. H. M. Minden, G. Milkereit and V. Vill, Chem. Phys. Lipids, 120 (2002) 45.
13 M. Fragata, A. Menikh and S. Robert, J. Phys. Chem., 97 (1993) 13920.
14 J. L. Nivea, A. Alonso, G. Basanez, F. M. Goni, A. Gulike, R. Vargas and V. Luzatti, FEBS Lett., 368 (1995) 143.
15 M. Salman, J. Deutsch, M. Tarshis, Y. Naot and S. Rottem, FEMS Microbiol. Lett., 123 (1994) 255.
16 G. Franzoso, D. S. Dimitrov, R. Blumenthal, M. F. Barile and S. Rottem, FEBS Lett., 303 (1992) 251.
17 M. Hato, H. Minamikawa, K. Tamada, T. Baba and Y. Tanabe, Adv. Colloid Interface Sci., 80 (1999) 233.
18 C. J. Drummond and D. Wells, Colloids Surf., A, 141 (1998) 131.
19 W. von Rybinski, Curr. Opin. Colloid Interface Sci., 1 (1996) 587.
20 K. Shinoda, A. Carlsson and B. Lindman, Adv. Colloid Interface Sci., 64 (1996) 253.
21 C. E. Fairhurst, S. Fuller, J. Gray, M. C. Holmes and G. J. Tiddy, In: Handbook of Liquid Crystals: D. Demus, J. W. Goodby, G. W. Gray, H.-W. Spiess, V. Vill, Eds; Wiley-VCH, Weinheim 1998, Vol. 3, p. 341.

22 L. J. Waters, S. A. Leharne and J. C. Mitchell, J. Therm. Anal. Cal., 80 (2005) 43.
23 E. Urbán, A. Bóta, B. Kocsis and K. J. Lohner, J. Therm. Anal. Cal., (2005) in press.
24 V. H. M. Minden, K. Brandenburg, U. Seydel, M. H. J. Koch, V. M. Garamus, R. Willumeit and V. Vill, Chem. Phys. Lipids, 106 (2000) 157.
25 H. B. Stuhrmann, N. Burkhardt, G. Dietrich, R. Jünemann, W. Meerwinck, M. Schmitt, J. Wadzack, R. Willumeit, J. Zhao and K. H. Nierhaus, Nucl. Instr. Meth., A356 (1995) 133.
26 G. D. Wignall and F. S. Bates, J. Appl. Crystallogr., 20 (1986) 28.
27 O. Glatter, J. Appl. Crystallogr., 10 (1977) 415.
28 J. S. Pedersen, Adv. Colloid Interface Sci., 70 (1997) 171.
29 L. A. Feigin and D. I. Svergun, Structure Analysis by Small-Angle X-Ray and Neutron Scattering, Plenum Press, New York 1987.

DOI: 10.1007/s10973-005-7250-2